Proceedings of the 2nd International Conference on Modern Medicine and Global Health
DOI: 10.54254/2753-8818/32/20240872

Lumican promotes gastric cancer progression by regulating the ERK pathway

Guangxi Liu[1], Xin Li[2], Xiaobing Shen[1, 3]

[1]School of Public Health, Southeast University, Nanjing, China,
[2]Jiangyin Center for Disease Control and Prevention, Jiangyin, China

[3]xb.shen@seu.edu.cn

Abstract. Globally, gastric cancer (GC) remains a major cause of death. Our prior study found lumican to be an important independent predictor of GC's poor overall survival and bioinformatics analysis suggested the MAPK pathway as a signaling cascade linked to lumican function. In our study, we observed that lumican exhibited a significant elevation in GC tissues and cells, hastening tumor proliferation in vivo in comparison to control groups. We also observed that knockdown of lumican effectively inhibited the proliferation, migration and invasion of AGS cells. On the contrary, overexpression of lumican promoted the proliferation, migration and invasion of AGS cells. We clarified that lumican was upstream of ERK in the MAPK pathway. In rescue assays, TBHQ further enhanced the promoting effect of lumican overexpression on cell migration and invasion and the increased expression of ERK 1/2 or p-ERK 1/2 levels. However, the increased expression of ERK 1/2 or p-ERK 1/2, migration and invasion were completely blocked by GDC-0994 in lumican–overexpressing AGS cells with TBHQ treated. Molecular docking prediction revealed that the amino acid sequence of lumican binding to ERK1/2 may also regulate the ERK pathway. In conclusions, lumican is highly expressed in GC and promotes the proliferation, migration and invasion of GC cells by regulating ERK pathway. Consequently, lumican emerges as pivotal indicators for both diagnosis and treatment in GC cases.

Keywords: gastric cancer, lumican, ERK signaling pathway.

1. Introduction

Based on recent statistics from the World Health Organization, gastric cancer (GC) ranks as the fifth most common and the fourth most lethal cancer worldwide [1]. The primary reason for mortality among GC patients is metastasis, predominantly through lymphatic and hematogenous pathways [2]. The covert nature and swift spread of GC result in a 5-year relative survival rate below 30% [3]. This situation underscores the urgency for research into the origins and development of GC to discover effective diagnostic and therapeutic methods, given the lack of preventive measures against GC's emergence and spread.

Lumican, a diminutive proteoglycan rich in leucine, belongs to the class II SLRP family and serves as an essential element of the extracellular matrix [4]. This molecule functions ambiguously in cancer development, acting as either a facilitator or a suppressor of tumor cell proliferation, motility, or infiltration [5, 6]. While lumican is implicated in the progression of esophageal [7], colorectal [8], and

DOI: 10.54254/2753-8818/32/20240872

lung cancers [9], it appears to hinder the growth of breast [10], pancreatic [11], and melanoma cancers [12]. Yet, its impact on the development, proliferation, and metastasis of GC remains under-explored.

Prior studies have underscored lumican to be an important independent predictor of GC's poor overall survival. Furthermore, bioinformatics evaluations have pointed to its prognostic relevance in GC, associating it with the mitogen-activated protein kinase (MAPK) signaling pathway [13]. Yet, these inferences, derived solely from bioinformatics, were not corroborated experimentally, leaving the precise molecular processes by which lumican impacts GC progression via the MAPK pathway ambiguous. This study delves deeper into lumican's oncogenic roles and its associated molecular pathways. We investigated the expression of lumican in GC patients and cell cultures, evaluating its effects on the proliferation, movement, and invasion of GC cells, while also delving into its association with the MAPK signaling pathway using rescue assays.

2. Materials and Approaches

2.1. Clinical tissue specimens

From May 2022 to August 2022, our research team acquired 22 sets of GC tissues along with their corresponding normal tissues, all originating from 22 distinct patients who were treated at ZhongDa Hospital. These tissue samples underwent a rigorous pathological examination to validate the diagnosis of GC before being surgically removed. Notably, none of the patients had undergone radiotherapy or chemotherapy prior to their surgical procedures, and there was no history of multiple malignant tumors among them.

2.2. Cell lines

In our research endeavor, we harnessed the GES-1 three distinct human GC cell lines: HGC-27, MKN45, and AGS (Key GEN, China). All the aforementioned cell lines were meticulously nurtured in RPMI 1640 medium (Thermo Fisher Scientific Inc, USA), which was supplemented with 10% fetal bovine serum (FBS, Thermo Fisher Scientific Inc, USA) and 1% penicillin-streptomycin (comprising 10,000 U/mL penicillin + 10,000 μg/mL streptomycin, Thermo Fisher Scientific Inc, USA), which we used in the refer to this medium here as complete medium. The cultivation of these cells transpired under precisely controlled conditions, specifically at a temperature of 37°C, within an environment enriched with 5% CO_2, within a dedicated carbon dioxide cell incubator [14].

2.3. siRNA transfection and lentivirus transduction

A lumican-targeting small inhibitory RNA (siRNA) was synthesized to knowndown lumican expression (Ruibo, China). Following standard naming conventions, the lumican-targeting siRNA was designated as si-lumican, while the negative control received the name nc-lumican. To facilitate lumican overexpression, the lumican gene sequence was integrated into the pHBLV vector (Hanbio, China), resulting in the creation of an overexpression vector named pLV-lumican. Simultaneously, an empty vector served as the negative control, termed pNC-lumican. The efficacy of the knockdown and overexpression model were confirmed by qRT-PCR and western blot analysis, which validated the successful diminution of lumican expression.

2.4. Quantitative real-time polymerase chain reaction (qRT–PCR)

For the assessment of lumican expression, both tissues and cells were initially subjected to RNA isolation employing TRIzol reagent (GenStar, China). Following this, cDNA was synthesized from the isolated lumican mRNA employing a reverse transcription kit (GenStar, China). The next step involved quantifying the lumican cDNA, which was executed employing a SYBR Green PCR Kit (GenStar, China), a widely recognized method for accurate and efficient quantification in molecular biology. These primers (Sangon Biotech, China) were specific to the lumican gene and the β-actin gene, which served as a control. The primer sequences were as detailed: for lumican, the forward primer sequence was 5'-GCTGCCAGAAGACAGTTTGG-3' and the reverse was 5'-

DOI: 10.54254/2753-8818/32/20240872

GGCACAAGCAACCTATCCAT-3'; for β-actin, the forward primer sequence was 5'-TCCATCATGAAGTGTGACGT-3' and the reverse was 5'-GAGCAATGATCTTGATCTTCAT-3'. These primers enabled the precise amplification of the target gene sequences, facilitating the subsequent analysis of lumican expression levels in the given samples.

2.5. Western blot

Cell lysates were prepared by utilizing RIPA lysis buffer (GenStar, China). The BCA protein assay kit was employed to quantify the protein content (Thermo Fisher Scientific Inc, USA). To analyze the proteins, equal quantities of proteins were subjected to separation through a 10.5% SDS-PAGE gel (Bio-Rad, USA). Subsequently, these proteins were transferred onto a PVDF (polyvinylidene fluoride) membrane (Millipore, USA). To mitigate non-specific binding, the membrane was initially treated with 5% skim milk powder. It then underwent an overnight incubation with primary antibodies, followed by a 1-hour incubation with secondary antibodies at room temperature, as detailed in reference [15]. To visualize the proteins, an enhanced chemiluminescence ECL substrate was utilized (Millipore, USA). Subsequently, the analysis of the blots was carried out using ImageJ software, a widely employed tool in the field of biological research for image analysis. The antibodies selected for use in this study for western blotting were specifically chosen due to their ability to target the desired proteins: lumican (1:1,000; catalog no. A11593; ABclonal, China), β-actin (1:1,000; catalog no. AC006; ABclonal, China), MEK1/2 (1:1,000; catalog no. #4694; CST, USA), p-MEK1/2 (1:1,000; catalog no. #9127; CST, USA), ERK1/2 (1:1,000; catalog no. #78241; CST, USA), and p-ERK1/2 (1:2,000; catalog no. #4370; CST, USA).

2.6. Cell counting kit-8 proliferation assay

In the context of this study, GC cells were cultivated within 96-well plates, each well accommodating 5,000 cells. These cells were nurtured in complete medium, with 100 μl each well at 37°C in carbon dioxide cell incubator, spanning time intervals of 24, 48, and 72 h. Following this phase, each well received a combined solution, including 10 μl cell counting kit-8 (CCK-8, Meilun, China) and 90 μl complete medium, for a time frame of 1h. The subsequent step involved the acquisition of optical density (OD) readings at a 450 nm wavelength (model Synergy4, produced by BioTek, USA).

2.7. Transwell assay

During the transwell assay for migration, 4×10^5/ml GC cells were introduced into the upper chambers in 200 μl of FBS-free RPMI-1640 medium. The bottom chambers of 24-well plates were filled with 600 μl of RPMI-1640 medium containing 20% FBS. After an incubation period of 24 h, media within the transwell upper chambers were carefully removed. Cells moved to the basement membrane were fixed with 2% paraformaldehyde for 20 min and subjected to a 15 –minute staining process using 1% crystal violet (Solarbio, China). A cotton swab was then gently wiped to remove cells that had not migrated on the Transwell basement membrane. Finally, Stained cells were photographed and counted in five randomly selected regions. In the transwell assay invasion, the chamber was coated with Matrigel (BD, USA), and the remaining steps were analogous to those of the migration assay [16].

2.8. Wound-healing assay

The process begins by cultivating GC cells in a 6-well dish until they form a dense, uninterrupted layer. Once this confluence is achieved, a sterile 200 μl pipette tip is employed to create a linear gap, mimicking a wound, followed by the removal of any cellular remnants with PBS. Subsequently, the cells are maintained in a RPMI-1640 growth medium. To evaluate cellular movement, images of three separate areas of the created wound are captured for each test group at two time points: initially (0 h) and after a 24-hour period. The extent of cell migration is quantified by comparing the change in the width of the wound from the initial measurement to that observed 24 h later. These measurements were reported as the migration distance, offering a quantifiable metric of the cells' migratory response to the tested factors.

DOI: 10.54254/2753-8818/32/20240872

2.9. Animal experiments

To assess lumican's role in cancer progression in vivo, we randomly allocated six BALB/c nude mice into two groups. One group received injections of AGS cells genetically modified to overexpress lumican via a lentiviral vector. The other group was injected with AGS cells carrying an empty lentiviral vector, serving as a control. These injections were administered into the right popliteal fossae of the mice. Tumor development was carefully tracked by periodically measuring the tumor's dimensions using calipers, with readings taken every three days. To determine tumor volume, the following formula was utilized: $V= L\times W^2/2$. Here, L denotes the tumor's longest diameter, while W represents its shortest dimension.

2.10. Immunohistochemistry (IHC)

All dissected tumors were fixed in a 4% paraformaldehyde solution. IHC assays were then carried out by Servicebio, a service provider based in China. Briefly, the procedure included paraffin embedding, deparaffinization with xylene, rehydration in graded ethanol, citric acid antigen retrieval, blocking endogenous peroxidase, blocking with serum, incubation with lumican antibody, visualization with diaminobenzidine, counterstaining with hematoxylin, final dehydration and mounting, microscopic examination, image acquisition, and analysis. The antibodies used for incubation were lumican (ABclonal, China).

2.11. Molecular docking

In our study, we utilized Uniprot and AlphaFold for protein annotation and structural analysis. Specifically, the structural data for lumican, ERK1, and ERK2 proteins were retrieved from Uniprot, with their respective PDB codes being P51884, P27361, and P28482. The interaction between lumican and the ERK1/2 proteins was then computationally simulated using AlphaFold2, a sophisticated tool for predicting protein structures. Following the docking simulation, the interactions and conformations of these proteins were visualized and analyzed using PyMOL, a powerful molecular visualization system.

2.12. Statistical analysis

In our investigation, each trial was meticulously replicated thrice to validate its consistency, with outcomes articulated as average values plus their associated standard deviations. Quantification of relative gene expression was executed through the $2^{-\Delta\Delta Ct}$ technique. For evaluating protein levels in western blots, cellular counts in transwell assays, outcomes from immunohistochemical studies, and findings from wound healing assays, we utilized ImageJ, an advanced image analysis tool. Comprehensive statistical examination of all amassed data was conducted utilizing Prism 8.0.

The decision to employ either a paired samples t-test or an independent samples t-test for two-group comparisons hinged on the specific attributes of the dataset. In instances necessitating the comparison of means across more than two groups, one-way ANOVA was the chosen method. This was supplemented by a post hoc Bonferroni test for detailed analysis of notable variances. We set the benchmark for statistical significance at $P< 0.05$, thereby affirming the robustness and relevance of our findings.

3. Results

3.1. Lumican was upregulated in GC tissues and cells.

In this study, examination of tissues revealed a notably elevated presence of lumican in cancerous tissues relative to normal tissues nearby (Figure 1A, $P< 0.001$). Furthermore, lumican's presence was substantially increased in various GC cell lines, specifically HGC-27, MKN45, and AGS, in contrast to GES-1 cells, which are benign. This difference is underscored by the statistical findings (Figure 1B, $P< 0.05$). These observations suggest a critical insight: heightened lumican expression emerges as a major indicator of negative outcomes in GC. It seems to correlate with more invasive tumor

DOI: 10.54254/2753-8818/32/20240872

characteristics and a less favorable prognosis. Notably, among all the GC cell lines examined in our study, AGS cells exhibited the highest lumican expression. This pronounced expression led us to select AGS cells for further experimental investigations, as they provide a relevant model for understanding the role of lumican in GC progression.

In addition, in order to investigate the function of lumican of GC, we transffected siRNA and lentivirus into AGS cells to establish knockdown and overexpression of lumican cell model. The effect of lumican- siRNA was observed by qRT-PCR and western blotting (Figure 2C and Figure 2E, $P< 0.001$). The effect of lumican- lentivirus was observed by qRT-PCR and western blotting (Figure 2D and Figure 2E, $P< 0.001$). These findings confirm that our approach to constructing the AGS cell model, through targeted lumican knockdown and overexpression, was effectively executed and successful.

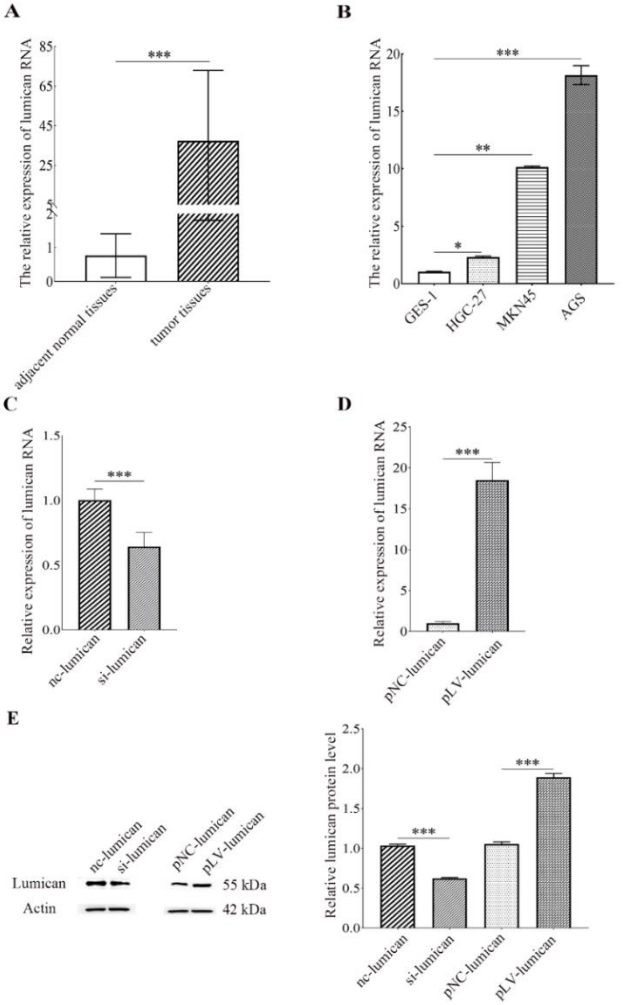

Figure 1. Expression of lumican in GC and GC cell models with lumican knockdown and over-expression.

(A) Comparative lumican expression analysis was conducted on 22 matched pairs of GC and adjacent normal tissues. The paired sample t-test was employed, utilizing the $2^{-\Delta\Delta CT}$ value for each sample pair. (B) qRT-PCR was employed to assess lumican expression across three GC cell lines and GES-1. (C) According to qRT-PCR analysis findings, transfection of lumican siRNA resulted in the downregulation of lumican expression in AGS cells. (D) As indicated by the qRT-PCR analysis, the transfection of lumican lentivirus led to an upregulation of lumican expression in AGS cells. (E) In the western blot assay, it was observed that the introduction of lumican siRNA led to a decrease in lumican levels, while the introduction of lumican lentivirus resulted in an increase of lumican in AGS cells. $*P< 0.05$, $**P< 0.01$, $***P< 0.001$.

3.2. Lumican influences the function of GC cells in vitro and in vivo.

To investigate the function of lumican in GC cells, we conducted CCK-8, tranwell, and wound healing assays using knockdown and overexpression techniques in AGS cell models. According to CCK-8 (Figure 2A, $P< 0.001$), transwell (Figure 2B and Figure 2C, $P< 0.001$), and wound healing (Figure 2D, $P< 0.001$) assays, interference of lumican decreased the proliferation, migration, and invasion of GC cells. Conversely, an augmentation in lumican expression was associated with enhanced proliferation (Figure 2E, $P< 0.001$), migration (Figure 2F and Figure 2H, $P< 0.001$), and invasion (Figure 2G, $P< 0.05$) of GC cells. The results obtained from experiments conducted in a laboratory setting strongly

DOI: 10.54254/2753-8818/32/20240872

indicate that lumican exerts a substantial influence on enhancing the proliferation, migration, and invasion of cells within the context of GC. This is indicative of lumican functioning as an oncogene in GC cells, contributing to the acceleration of GC cells growth and metastasis.

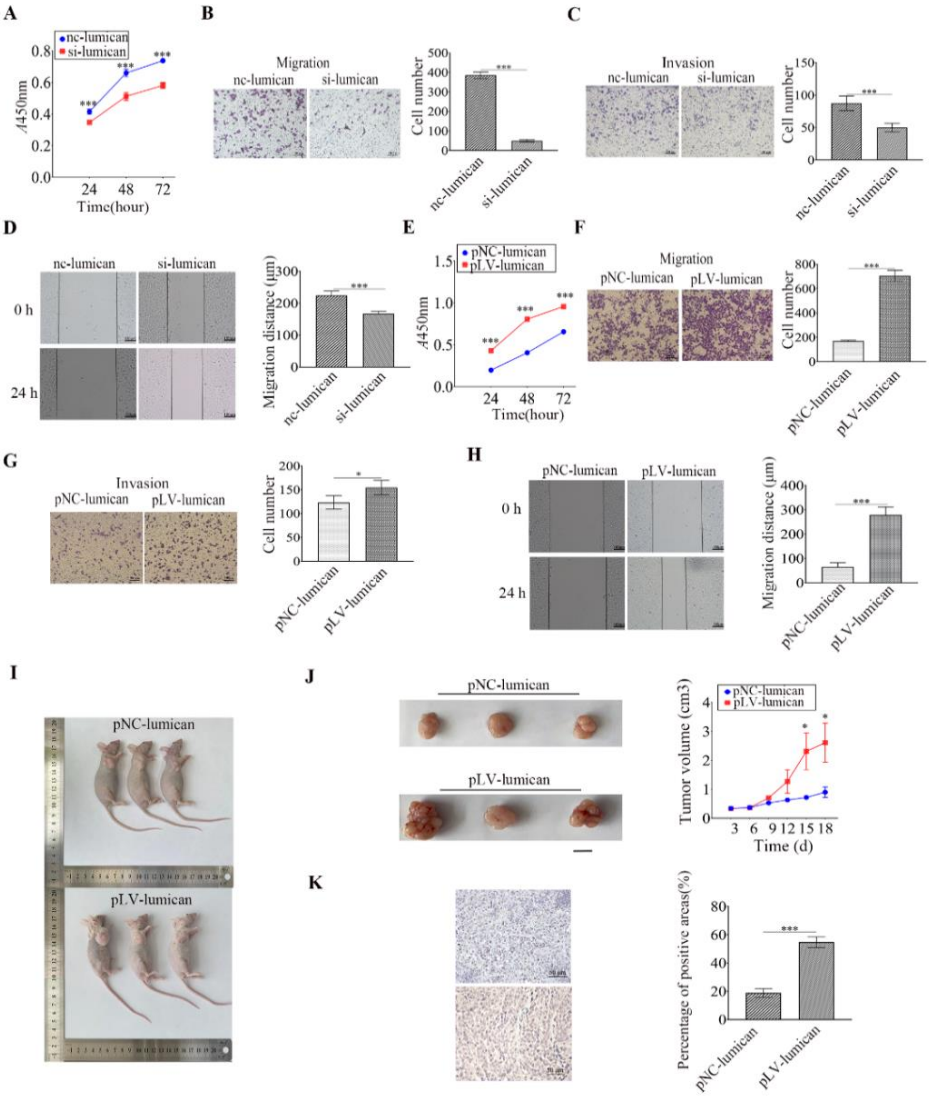

Figure 2. The function of lumican in vitro and in vivo.

(A) Transfection of lumican siRNA reduced AGS cells proliferation rates in CCK-8 assays. (B) Transfection of lumican siRNA reduced invasive AGS cell number in Transwell assays for invasion. (C) Transfection of lumican siRNA reduced migrative AGS cell number in Transwell assays for migration. (D) Transfection of lumican siRNA reduced AGS cells migration distances in Wound-healing assays. (E) According to the CCK-8 assay, transfection of lumican lentiviral increased AGS cells proliferation rates. (F) Transfection of lumican lentiviral increased invasive AGS cell number in Transwell assays for invasion. (G) Transfection of lumican lentiviral increased migrative AGS cell number in Transwell assays for migration. (H) Transfection of lumican lentiviral increased AGS cells migration distances in wound-healing assays. Samples from B to H were photographed using a 100* magnification, with a scale bar equivalent to 100 micrometers, scale bar = 100 μm. (I)-(J) Subcutaneous tumorigenesis model, overexpression lumican significantly increased tumour growth compared to its control in vivo, scale bar is 1 cm. (K) IHC assay demonstrated the level of lumican in pNC-lumican and pLV-lumican-treated groups, scale bar is 50 μm. *P< 0.05, **P< 0.01, ***P< 0.001.

DOI: 10.54254/2753-8818/32/20240872

To extend these findings to an in vivo context, we established a subcutaneous tumorigenesis model using AGS cells that stably expressed lumican, introduced via lentiviral transduction (Figure 2I, $P< 0.001$). The results obtained from this model align with our observations in the laboratory setting. In the context of nude mice, it was evident that the tumors originating from cells that had been injected with a lentivirus expressing lumican (pLV-lumican) exhibited markedly reduced volume in comparison to those arising from the negative control group (pNC-lumican) (Figure 2J, $P< 0.05$). Furthermore, there was a substantial increase in lumican expression levels within the pLV-lumican group when contrasted with the pNC-lumican group (Figure 2K, $P< 0.001$).

Collectively, these discoveries underscore the potential of lumican as a promising therapeutic target. This is particularly noteworthy given its substantial involvement in fostering the proliferation and invasiveness of GC.

3.3. The association between lumican and the ERK pathway.

In our previous research, we discovered that lumican may potentially trigger the activation of the MAPK pathway in GC cells [13]. To further investigate this phenomenon, we utilized western blot analysis to determine the levels of extracellular signal-regulated kinase 1/2 (ERK1/2), its phosphorylated form (p-ERK1/2), mitogen-activated protein kinase kinase (MEK1/2), and phosphorylated MEK1/2 (p-MEK1/2) proteins in AGS cells. Our observations unveiled a significant decrease in the levels of both ERK1/2 and p-ERK1/2, with interference of lumican, in stark contrast to their augmentation when lumican levels were overexpressed (Figure 3A, $P< 0.001$). However, alterations in lumican did not significantly influence MEK1/2 or p-MEK1/2 in this cellular context (Figure 3A, $P> 0.05$). These findings imply that lumican suppression leads to deactivation of the ERK signaling in GC AGS cells. Consequently, we selected ERK modulators, both inhibitors and activators, for further rescue assays to explore the regulatory relationship between lumican and ERK1/2.

Next, we delved into the specific amounts of the ERK inhibitor (GDC-0994) and its activator (TBHQ) employed in various rescue assays. To determine the optimal concentration of GDC-0994, we conducted CCK-8 assays. Our focus was to identify the concentration at which AGS cells, enhanced by lumican overexpression, would resume proliferation at the same rate as the baseline control cells. It was established that the ideal concentration for GDC-0994 was 10 μM, as illustrated in Figure 4B ($P> 0.05$). Furthermore, referencing prior studies, we determined that the optimal concentration for the ERK activator TBHQ should also be set at 10 μM, as cited in references [17, 18].

In rescue assays, TBHQ further increased in ERK1/2 and p-ERK1/2 levels in AGS cells with overexpressing lumican (Figure 3C, $P< 0.001$). In contrast, the increased expression of ERK 1/2 and p-ERK 1/2 was completely blocked by GDC-0994 in overexpressing lumican AGS cells, also treated with TBHQ (Figure 3C, $P< 0.001$). These findings strongly suggest that lumican positively regulates ERK, positioning ERK downstream in the MAPK pathway. Further, TBHQ was observed to amplify the impact of lumican overexpression on AGS cell migration and invasion (Figures 3D-E, $P< 0.001$), affirming its role in promoting these cellular behaviors. However, when these lumican-enhanced AGS cells were treated with TBHQ and GDC-0994, the migration and invasion processes were completely hindered (Figures 3D-E, $P< 0.001$). This leads to the conclusion that ERK, functioning downstream of lumican, is integral to the expression and biological activity within GC cells. Thus, lumican, through its influence on ERK, can significantly drive the development of GC cells.

For an in-depth exploration of the interactions between lumican and ERK1/2, we employed AlphaFold to construct 3D models of lumican, ERK1, and ERK2, as illustrated in Figure 3F. Subsequently, these proteins underwent molecular docking to identify the specific amino acid residues in lumican, ERK1, and ERK2 that engage in interactions, shown in Figure 3G and Table 1. Predominantly, hydrogen bonds facilitated these protein-protein interactions. Serving as an antecedent to ERK1/2, the amino acid sequence of lumican, which interacts with ERK1/2, might have a pivotal function in controlling the ERK pathway. Our investigation underscores lumican as a prospective candidate for crafting a pharmaceutical agent aimed at overseeing the ERK pathway, which could potentially usher in a groundbreaking shift in the strategy for treating GC.

DOI: 10.54254/2753-8818/32/20240872

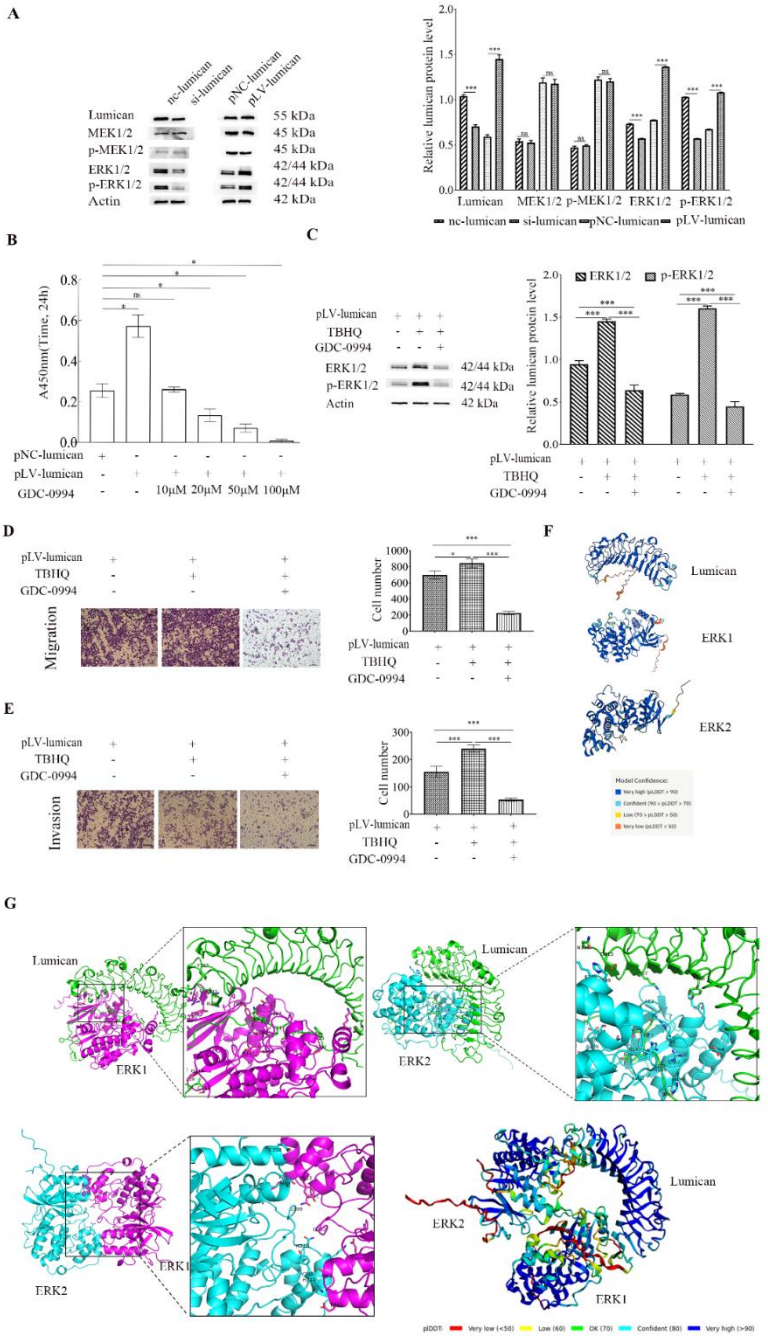

Figure 3. Mechanisms of lumican interaction with ERK1/2.

(A) Western blot assays revealed the quantities of MEK1/2 or phosphorylated MEK1/2, as well as ERK 1/2 or phosphorylated ERK 1/2 in AGS cell culture subsequent to the introduction of siRNA or its control, and a lentiviral vector or its corresponding void counterpart. (B) Utilization of the CCK-8 assay for determining the optimal concentrations of an ERK inhibitor. (C) The results obtained from the western blot assays reveal the measurements of ERK 1/2 and the phosphorylated form of ERK 1/2 after rescue assays. (D) Transwell assays for migration after rescue assays. (E) Transwell assays for invasion after rescue assays. (All samples above were imaged at 100× magnification. Scale bar = 100 μm). (F) Predicted protein structures of lumican, ERK1 and ERK2. (G) Molecular docking visualization results. ns $P > 0.05$, *$P < 0.05$, **$P < 0.01$, ***$P < 0.001$.

DOI: 10.54254/2753-8818/32/20240872

Table 1. Elaborate amino acid interaction patterns in the protein molecular docking models of lumican-ERK1, lumican-ERK2, and ERK1-ERK2.

Lumican-ERK1		**Lumica-ERK2**		**ERK1-ERK2**	
Lumican-Residue	ERK1-Residue	Lumican-Residue	ERK2-Residue	ERK1-Residue	ERK2-Residue
MET1	ASP321	LEU8	CYS178	TYR250	GLU62
LEU8	THR159	LEU8	THR176	ASN218	GLY182
LEU8	CYS161	ILE13	GLU126	LYS276	GLU334
GLN19	THR190	THR16	SER170	GLY199	ASN201
GLN19	TYR187	THR16	ASP128	GLN79	TYR233
TYR20	TYR36	GLN19	ASP166	GLU315	LYS259
TYR23	LEU184	TYR20	ASP184	LYS276	GLU334
TYR23	LEU170	TYR20	ASN171	HIS249	GLU341
ASP24	TYR205	ASP22	LEU163	GLU368	HIS232
ASP24	ILE198	ASP24	ASN161	GLU351	LYS259
PHE25	ASN201	PRO26	ASP192		
PHE25	SER202	LYS120	ASP354		
LYS307	ALA35	LYS307	ALA52		
PHE6	CYS161	PHE6	CYS178		
PHE9	GLN119	PHE9	GLN136		
GLN19	LYS151	GLY15	GLU50		
GLN19	THR190	GLY18	LYS71		
GLN19	THR193	GLN19	ARG84		
TYR21	TYR195	ASP22	LEU163		
TYR23	LEU184	ASP22	ARG165		
ASN75	LYS259	TYR233	HIS78		
TYR303	GLN17	MET1	ASP338		
ALA332	ARG15	LYS120	ASP354		
ASN333	TYR30	ASP22	ARG87		
		ASP22	ARG189		
		ASP22	ARG165		
		ASP24	HIS197		
		ASP312	HIS249		
		ASN338	LYS248		

4. Discussion

The etiology and progression of GC represent intricate, multi-stage phenomena, necessitating the aggregation of numerous genetic alterations [19]. Prompt detection and vigorous intervention markedly enhance the survival rates of individuals afflicted with GC [20]. Consequently, identifying novel biomarkers is pivotal for refining the therapeutic approaches for GC. Our preceding bioinformatics examination identified lumican as a significant prognostic element in GC cases [13]. Lumican exhibits pronounced expression across various cancerous tissues and cell lines. Notably, lumican is conspicuously present in pancreatic cancer tissues and cell lines (namely PK-8 and MIA-PaCa-2) [21], and it demonstrates elevated levels in cervical cancer tissues and cell lines (including CaSki, ME-180, and HeLa) [22]. Consequently, augmented lumican expression might be indicative of more aggressive cancerous behaviors and dismal prognoses, making lumican evaluation a potential tool in forecasting patient outcomes and shaping therapeutic strategies. Our clinical data analysis links poor prognosis in patients with elevated lumican levels. Furthermore, within our lumican-overexpressing nude mouse model, the cohort featuring elevated lumican expression displayed a marked augmentation in tumor dimensions in contrast to the control cohort. This suggests that lumican

DOI: 10.54254/2753-8818/32/20240872

might emerge as a promising target for therapeutic intervention in cases of GC. Our investigation underscores the significance of heightened lumican expression as a substantial hazard factor for reduced survival rates among GC patients by experimental evidence.

Lumican exerts a dual influence on the dynamics of cancer, alternately expediting or retarding the proliferation, movement, and infiltration of malignant cells. This impact on the progression of tumors can either be positive or negative [5, 6]. To elaborate, lumican augments the migratory and invasive capacities of neuronal cancer cells by operating through the lumican/FOXO3 pathway [23]. In contrast, diminished lumican levels curb the migration and infiltration of hepatocellular carcinoma cells, ascribed to the inhibition of the ERK/JNK pathway [24]. In the context of breast cancer cells, lumican downregulates the phosphorylation of ERK1/2 within the MAPK signaling pathway, subsequently hampering their proliferation, movement, and infiltration [10] .However, the attenuation of tumor growth, mobility, invasion, proliferation, and adhesion in esophageal, pulmonary, and melanoma cancer cells has been attributed to the reduced expression of lumican [25, 7, 9]. Cancer-associated fibroblasts (CAFs), residing within the tumor stroma that encircles the malignant cells, play a pivotal role in mediating lumican's involvement in the genesis and spread of GC [26]. Our research findings unveil that lumican plays a direct role in promoting the proliferation, migration, and invasion of GC cells, as evidenced by our in vitro functional experiments. Contrasting with existing literature, our study further elucidates lumican's role in GC as a promoter of cancerous activity directly.

In prior literature, lumican's potential to influence downstream signalling pathways has been posited. Building upon this and our preceding bioinformatics analyses, we delved into lumican's role in augmenting GC via the MAPK pathway. Lumican, known to promote cancer via the ERK pathway across various cancer types, was further scrutinized. In bladder cancer (BCa) cells, reducing lumican levels, followed by diminished MEK and ERK expression within the MAPK pathway, led to reduced BCa cell migration and triggered cell cycle arrest [27]. In the context of colon cancer, the inhibition of lumican expression, achieved through epigenetic adjustments in the ERK signaling pathway, effectively arrested the movement of cancer cells in laboratory settings as well as within living organisms [28]. Of the MAPK pathways, the MEK–ERK signaling sequence has been most comprehensively studied to date [29, 30]. Our current research reveals lumican elevating ERK but not MEK levels in GC, suggesting its mechanism of action might be situated upstream of ERK in the MEK-ERK cascade. In subsequent rescue experiments, it was further confirmed that lumican facilitates the migration and infiltration of GC cells by triggering the ERK pathway. These findings demonstrate similarities with mechanisms identified in cases of colon cancer [28]. We thus present the novel finding that lumican fosters GC development through the ERK pathway. Our findings offer fresh perspectives on lumican's role in cancer genesis and progression, suggesting that lumican expression and ERK pathway activation status could inform patient classification and tailored treatments. Particularly, patients exhibiting high lumican expression coupled with intense ERK pathway activity might benefit from therapies specifically designed to inhibit this pathway.

However, there are some limitations to this study. First, we chose one of the three cell lines (HGC-27, MKN-45, and AGS) as representative for functional and mechanistic exploration. This may not be sufficient to validate our conclusions. Other cell lines commonly used for GC studies could be used to further support our conclusions. Furthermore, although a predicted amino acid sequence of lumican can interact with ERK1/2, the accuracy of this sequence necessitates further verification, and the investigation of lumican as a potential drug demands a prolonged process.

5. Couclusion

In summary, our investigation has unveiled a significant rise in the manifestation of lumican in GC, affecting the advancement of GC both within laboratory settings and within living organisms. This heightened lumican expression demonstrates an inverse correlation with patient prognoses, underscoring its potential as a predictive indicator. Furthermore, lumican's capability to regulate the downstream ERK signaling pathway holds considerable importance, particularly in light of the identified sequence of amino acids within lumican that interacts with ERK1/2. This interaction hints at

DOI: 10.54254/2753-8818/32/20240872

its ability to exert influence over the ERK pathway, shedding light on lumican's involvement in the molecular underpinnings of GC and its prospective utility as a target for therapeutic intervention.

References

[1] Sung, Ferlay, Siegel *et al.* (2021). Global Cancer Statistics 2020: GLOBOCAN Estimates of Incidence and Mortality Worldwide for 36 Cancers in 185 Countries. CA Cancer J Clin, 71 (3), pp. 209-249

[2] Yin, Ji, and Shen. (2003). Relationship between lymph node sinuses with blood and lymphatic metastasis of gastric cancer. World J Gastroenterol, 9 (1), pp. 40-43

[3] Allemani, Matsuda, Di Carlo *et al.* (2018). Global surveillance of trends in cancer survival 2000-14 (CONCORD-3): analysis of individual records for 37 513 025 patients diagnosed with one of 18 cancers from 322 population-based registries in 71 countries. Lancet, 391 (10125), pp. 1023-1075

[4] Karamanou, Perrot, Maquart *et al.* (2018). Lumican as a multivalent effector in wound healing. Adv Drug Deliv Rev, 129, pp. 344-351

[5] Appunni, Rubens, Ramamoorthy *et al.* (2021). Lumican, pro-tumorigenic or anti-tumorigenic: A conundrum. Clin Chim Acta, 514, pp. 1-7

[6] Giatagana, Berdiaki, Tsatsakis *et al.* (2021). Lumican in Carcinogenesis-Revisited. Biomolecules, 11 (9)

[7] Yamauchi, Kanke, Saito *et al.* (2021). Stromal expression of cancer-associated fibroblast-related molecules, versican and lumican, is strongly associated with worse relapse-free and overall survival times in patients with esophageal squamous cell carcinoma. Oncol Lett, 21 (6)

[8] de Wit, Carvalho, Delis-van Diemen *et al.* (2017). Lumican and versican protein expression are associated with colorectal adenoma-to-carcinoma progression. PLoS One, 12 (5), pp. e0174768

[9] Yang, Li, Chu *et al.* (2018). Downregulation of lumican accelerates lung cancer cell invasion through p120 catenin. Cell Death Dis, 9 (4), pp. 414

[10] Karamanou, Franchi, Onisto *et al.* (2020). Evaluation of lumican effects on morphology of invading breast cancer cells, expression of integrins and downstream signaling. FEBS J, 287 (22), pp. 4862-4880

[11] Li, Lee, Kang *et al.* (2019). Hypoxia-induced autophagy of stellate cells inhibits expression and secretion of lumican into microenvironment of pancreatic ductal adenocarcinoma. Cell Death Differ, 26 (2), pp. 382-393

[12] Brezillon, Untereiner, Mohamed *et al.* (2020). Label-Free Infrared Spectral Histology of Skin Tissue Part II: Impact of a Lumican-Derived Peptide on Melanoma Growth. Front Cell Dev Biol, 8, pp. 377

[13] Chen, Li, Hu *et al.* (2020). LUM Expression and Its Prognostic Significance in Gastric Cancer. Front Oncol, 10

[14] Jiang, Hu, Cao *et al.* (2022). Hsa_circ_0000081 promotes the function of gastric cancer through sponging hsa-miR-423-5p to influence 3-phosphoinositide-dependent kinase 1 expression. Bioengineered, 13 (4), pp. 8277-8290

[15] Zhang, Li, and Hu. (2018). Exosomal transfer of miR-214 mediates gefitinib resistance in non-small cell lung cancer. Biochem Biophys Res Commun, 507 (1-4), pp. 457-464

[16] Stoellinger, and Alexanian. (2022). Modifications to the Transwell Migration/Invasion Assay Method That Eases Assay Performance and Improves the Accuracy. Assay Drug Dev Techn, 20 (2), pp. 75-82

[17] Li, Li, Lan *et al.* (2022). Damnacanthal isolated from morinda species inhibited ovarian cancer cell proliferation and migration through activating autophagy. Phytomedicine, 100

[18] Miyauchi, Nakamura, Furukawa *et al.* (2002). Promoting effects of combined antioxidant and sodium nitrite treatment on forestomach carcinogenesis in rats after initiation with N-methyl-N'-nitro-N-nitrosoguanidine. Cancer Lett, 178 (1), pp. 19-24

DOI: 10.54254/2753-8818/32/20240872

[19] Moreira, Pereira, Melo *et al.* (2020). The Extracellular Matrix: An Accomplice in Gastric Cancer Development and Progression. Cells, 9 (2)
[20] Nie, Wu, Yu *et al.* (2017). A global burden of gastric cancer: the major impact of China. Expert Rev Gastroenterol Hepatol, 11 (7), pp. 651-661
[21] Ping Lu, Ishiwata, and Asano. (2002). Lumican expression in alpha cells of islets in pancreas and pancreatic cancer cells. J Pathol, 196 (3), pp. 324-330
[22] Naito, Ishiwata, Kurban *et al.* (2002). Expression and accumulation of lumican protein in uterine cervical cancer cells at the periphery of cancer nests. Int J Oncol, 20 (5), pp. 943-948
[23] Salcher, Spoden, Huber *et al.* (2019). Repaglinide Silences the FOXO3/Lumican Axis and Represses the Associated Metastatic Potential of Neuronal Cancer Cells. Cells, 9 (1)
[24] Mu, He, Hou *et al.* (2018). [nterference of Lumican Regulates the Invasion and Migration of Liver Cancer Cells. Sichuan Da Xue Xue Bao Yi Xue Ban, 49 (3), pp. 358-363
[25] Jeanne, Untereiner, Perreau *et al.* (2017). Lumican delays melanoma growth in mice and drives tumor molecular assembly as well as response to matrix-targeted TAX2 therapeutic peptide. Sci Rep, 7 (1), pp. 7700
[26] Kolch. (2005). Coordinating ERK/MAPK signalling through scaffolds and inhibitors. Nat Rev Mol Cell Biol, 6 (11), pp. 827-837
[27] Mao, Luo, Huang *et al.* (2019). Knockdown of Lumican Inhibits Proliferation and Migration of Bladder Cancer. Transl Oncol, 12 (8), pp. 1072-1078
[28] Quan, Chen, Hao *et al.* (2017). Epigenetic silence of lumican inhibits the motility of colon cancer via inactivating MAPK signaling in vitro and in vivo. Int J Clin Exp Med, 10 (6), pp. 8875-8883
[29] Montagut, and Settleman. (2009). Targeting the RAF-MEK-ERK pathway in cancer therapy. Cancer Letters, 283 (2), pp. 125-134
[30] Ullah, Yin, Snell *et al.* (2022). RAF-MEK-ERK pathway in cancer evolution and treatment. Semin Cancer Biol, 85, pp. 123-154